Pergamon

Bioorganic & Medicinal Chemistry 6 (1998) 1857–1863

BIOORGANIC & MEDICINAL CHEMISTRY

Effect of 2′-OH Acetylation on the Bioactivity and Conformation of 7-*O*-[*N*-(4′-Fluoresceincarbonyl)-L-alanyl]taxol. A NMR-fluorescence Microscopy Study

Jesús Jiménez-Barbero,[a] André A. Souto,[a] Miguel Abal,[b] Isabel Barasoain,[b] Juan A. Evangelio,[b] A. Ulises Acuña,[c] José M. Andreu[b] and Francisco Amat-Guerri[a,*]

[a]*Instituto de Química Orgánica, CSIC, Juan de la Cierva 3, E-28006 Madrid, Spain*
[b]*Centro de Investigaciones Biológicas, CSIC, Velazquez 144, E-28006 Madrid, Spain*
[c]*Instituto de Química-Física Rocasolano, CSIC, Serrano 119, E-28006 Madrid, Spain*

Received 11 March 1998; accepted 26 May 1998

Abstract—The relationship between conformation, 2′-OH acetylation, and bioactivity of two fluorescent taxoids has been investigated by a combination of NMR and fluorescence microscopy techniques. These taxoids present the structure of taxol with the 7-OH group esterified with the *N*-(4′-fluoresceincarbonyl)-L-alanine group and with the 2′-OH group free (taxoid **2**) or acetylated (taxoid **3**). The larger water solubility of **2** and **3** compared with taxol allowed a detailed NMR study in DMSO-d_6/D_2O (3/7), showing that both taxoids adopt a similar collapsed conformation in which the hydrophobic groups 2-*O*-benzoyl, 3′-phenyl and 4-*O*-acetyl are in close proximity, with the fluorescein group displaying unrestricted motion. On the other hand, while taxoid **2** retains essentially the ability of taxol to induce in vitro microtubule assembly and to bind to cell microtubules, the 2′-acetylated derivative **3** does not show immediate activity. However, when taxoid **3** is left in the cell culture, the slow hydrolysis of the 2′-acetate group in the medium liberates the cytotoxic, microtubule-specific taxoid **2**. The intense emission of this active derivative (**2**) allows the accurate recording of the drug-cell interaction from the very initial steps using fluorescence microscopy. These experiments show conclusively, for the first time in cell cultures, that a free 2′-OH group in taxol is essential for the recognition of the drug by the binding site of cellular microtubules.

Introduction

The natural diterpenoid paclitaxel (Taxol®, **1**) is one of the most effective drugs in the therapy of ovarian cancer,[1] metastatic breast cancer, head and neck cancer, and lung cancer.[2] Its bioactivity is connected with the binding of the drug to microtubules of the cytoskeleton,[3] but the details of this interaction at a molecular level are largely unknown. From studies of the structure–activity relationship of taxol and analogues,[4] it has been demonstrated that the side chain at the position 13 and the stereochemistry of the groups at positions 2′ and 3′ are crucial for the biological activity. Moreover, it has been reported that esterification of the 2′-OH group with carboxylic acids results in loss of the in vitro interaction with microtubules in solution but, interestingly, the cell cytotoxicity is retained.[5] This paradoxical observation might be understood if the hydrolysis of the acetate group takes place within the cells, an explanation also supported by the observation that taxol derivatives with the 2′-OH group replaced by H, F or OMe show 70–200 times lower cytotoxicity.[6] The therapeutical relevance of the 2′-OH group, and the possible in vivo hydrolysis of its esters, triggered several syntheses of taxol prodrugs modified at this position.[7] However, to our knowledge no detailed studies on the place where these prodrugs are hydrolyzed in cultures of living cells have been reported.

A further essential aspect related with the bioactivity of taxol is the 3-D conformation of the drug, both in aqueous solution and bound to tubulin, the protein that forms microtubules. The solution conformation of taxol

Key words: Fluorescence; NMR; microtubule probes; paclitaxel structure–activity relationship.
*Corresponding author. Fax: +34-91-5644853; E-mail: famat@fresno.csic.es

0968-0896/98/$—see front matter
PII: S0968-0896(98)00149-7

has been elucidated by NMR spectroscopy both in chloroform[8] and in methylene chloride,[9] but not in water because of the low solubility of the drug. In the cited solvents taxol forms aggregates stabilized through intermolecular H-bonds, with a monomer unit in a folded conformation where interactions between aromatic protons do not take place. It has been speculated[10] that this conformation might be similar to that at the microtubule binding site. In DMSO/water mixtures the taxol molecule adopts a very different conformation, characterized by a hydrophobic clustering ('hydrophobic collapse') involving the 2-*O*-benzoyl, 3′-phenyl and 4-*O*-acetyl groups.[11] Interestingly, one of the two conformers observed in the X-ray crystal structures of taxol[12] and 10-deacetyl-7-*epi*taxol[13] also shows this collapsed form. The same structure has been observed in other active taxoids in similar solvent mixtures.[14–16] A water soluble 7-OH ether of taxol with the group 2-(*N*-methyl)pyridinium acetate and with in vitro cytotoxicity similar to that of taxol has shown the same clustering in D_2O solution.[17] On the other hand, the same collapsed conformation has been observed for the in vitro-inactive 2′-*O*-acetyltaxol in 1/1 DMSO/water solution,[18] suggesting that the 2′-OH group does not take part in the collapse, although it is essential for the bioactivity of the drug.

As a part of our current studies on the mechanism of taxol interaction with microtubules,[19] we have previously described[20] the synthesis of a fluorescent, water soluble taxoid with a fluorescein chromophore linked through an L-alanine spacer at the position 7 (compound **2**, see formulas). Using an alanine ester at the 7-OH as a general linker with an easily reactive NH_2 group facilitates the derivatization of the drug. This synthetic strategy has also been reproduced with success in other laboratories.[21] Taxoid **2** shows essentially the same bioactivity as the parent drug and has allowed for the first time the direct visualization of the cell microtubule system by fluorescence microscopy of diverse normal and malignant cells, providing new methods for the study of the molecular mechanism of taxoid-induced microtubule assembly and of the structure–activity relationship of the drug.[20,22] The present work is an application of the fluorescence microscopy technique to investigate at the cellular level the effect of two structural parameters—conformation and 2′-OH acetylation—on the taxol activity. With this purpose we report the 3-D solution

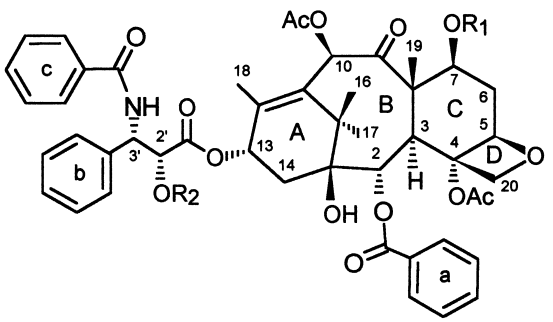

1 (taxol): $R_1 = R_2 = H$

2: R_1 = fluoresceinalanyl, $R_2 = H$

3: R_1 = fluoresceinalanyl, R_2 = COMe

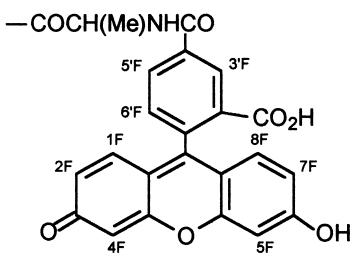

fluoresceinalanyl fluorophore

Table 1. NOEs and their intensities (s, strong; m, medium; w, weak) in the NOESY spectra of the fluorescent taxoids **2** and **3** in 3:7 v/v DMSO-d_6/D_2O (600 MHz, 5–25 °C)

Proton pair		Proton pair	
o-H(a)/*m*-H(b)	m	4-MeCO/H-13	w
o-H(a)/*p*-H(b)	w	4-MeCO/H-14a	m
o-H(a)/4-MeCO	s	4-MeCO/H-14b	m
o-H(a)/H-14a	m	4-MeCO/H-20a	w
o-H(a)/H-14b	m	4-MeCO/H-2′	s
o-H(a)/H-17	m	4-MeCO/H-3′	m
o-H(a)/H-20a	s	H-5/H-6a	m
o-H(a)/H-20b	s	H-5/H-6b	m
m-H(a)/*m*-H(b)	m	H-5/H-7	s
m-H(a)/*p*-H(b)	w	H-5/H-18,H-19	w
m-H(a)/4-MeCO	w	H-5/H-20a	m
o-H(b)/H-13	w	H-5/H-20b	m
o-H(b)/H-14a	s	H-6a/H-7	s
o-H(b)/H-14b	s	H-6a/H-10	w
o-H(b)/H-2′	m	H-6b/H-7	m
o-H(b)/H-3′	s	H-6b/H-19	s
m-H(b)/4-MeCO	s	H-7/H-10	s
H-2/H-3	s	H-7/Me(Ala)	w
H-2/H-13	w	H-10/10-MeCO	w
H-2/H-16	s	H-10/H-16	m
H-2/H-19	s	H-10/H-18,H-19	s
H-2(7)/H-20a	s	H-10/H-20a	w
H-2(7)/H-20b	s	H-10/Me(Ala)	w
H-3/4-MeCO	m	10-MeCO/H-16	m
H-3/H-6b	m	10-MeCO/Me(Ala)	m
H-3/H-10	s	H-13/H-14a	s
H-3/H-13	w	H-13/H-14b	s
H-3/H-14a	m	H-13/H-17	s
H-3/H-14b	m	H-14a/H-2′	w
H-3/H-19	m	H-14a/H-3′	w
H-3/H-20a	w	H-16/H-20a,H-20b	m
H-3/H-20b	w	H-19/H-20a	s
H-3/Me(Ala)	w	H-2′/H-3′	m
4-MeCO/H-5	m	Me(Ala)/H(Ala)	s
4-MeCO/H-7	w	Me(Ala)/H-3′F,H-5′F	m

structure of **2** and its 2′-*O*-acetyl derivative **3**, as models of taxol and its 2′-*O*-acetylated derivative, but both with larger water solubility and high intrinsic fluorescence quantum yield. These properties give the unique opportunity to obtain accurate NMR data of a bioactive taxoid in an aqueous environment, and to resolve in time and space the interactions with the cytoskeleton.

Results and Discussion

Conformational analysis

The proton chemical shifts and the coupling constants of the fluorescent taxoids **2** and **3** were recorded in 3/7 v/v DMSO-d_6/D_2O. The resonance signals of the taxol moiety were assigned by comparison with the reported assignments for a similar taxoid in water,[17] assisted by COSY, TOCSY and NOESY experiments. The signals were independent of temperature in the 25–50 °C range.

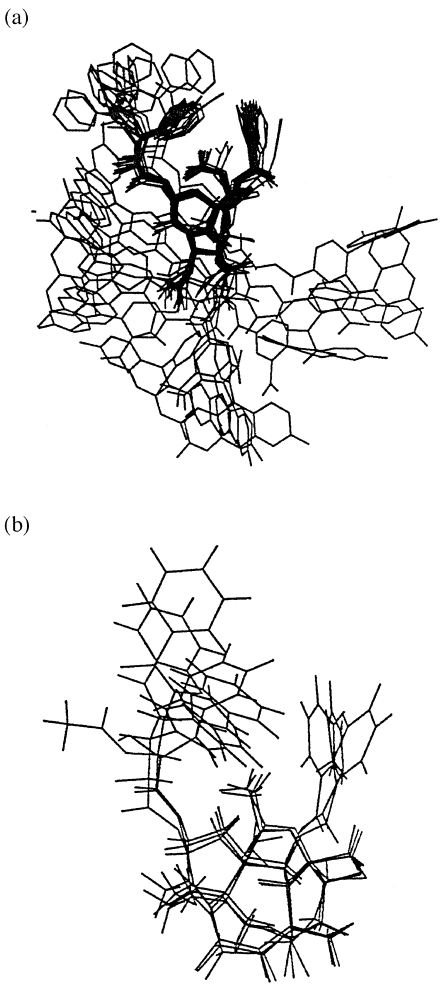

Figure 1. Equilibrium conformation in 3/7 DMSO-d_6/D_2O of the fluorescent taxoid **2** (panel a), and the overlay of this structure with that of taxoid **3** and with that of a water-soluble 7-OH ether of taxol[17] (panel b). The 7-fluoresceinalanyl group of **2** and **3**, and the ether group of the taxol ether, have been omitted for clarity.

NOESY experiments were used in a subsequent step to generate 3-D structures. The NOEs listed in Table 1 indicate the same average conformation for taxoids **2** and **3** in this solvent. Seventy NOEs were unambiguously assigned to specific proton pairs and translated into distance constraints. The strong NOEs between H-13 and 17-Me, and between H-7 and H-10 indicate that the A and B rings (see formulas) present boat and chair–boat conformations, respectively. The observed key NOEs between the protons in the groups 2-OBz, 3′-Ph and 4-OAc are remarkably similar to those described previously for the hydrophobic clustering of these groups in related taxoids in aqueous solvents.[11,16–18] Additional evidence for the side chain conformation required for hydrophobic contacts Ar-Ar-Me came from the value of the $J_{2'3'}$ coupling constant (7.5 Hz in both compounds), indicating a nearly *trans* relationship between H-2′ and H-3′.

A superposition of 10 structures of **2** with no violations is shown in Figure 1(a). It is interesting that while the molecular core is well defined, the fluorescein group may adopt a variety of orientations with respect to the main skeleton, consistent with the lack of observed NOEs for this region. Some minor movements of the aromatic and the 4-OAc groups are still possible and compatible with the NOE data. Taxoid **3** has basically the same conformation as **2** (not shown), and the same hydrophobic clustering is also evident.

As noted above, the hydrophobic clustering of the taxol core observed herein for taxoids **2** and **3** parallels that previously described for a variety of taxol derivatives,[11,16–18] in spite of the presence of the large fluorescein group. In fact, the overlay of the structures of **2** and **3** with that of the 7-*O*-[2-(*N*-methyl)pyridinium] salt of taxol[17] yields a close alignment (Fig. 1(b)).

Interactions with microtubules

The bioactivity of taxoids **2** and **3** was tested by placing a tubulin solution under conditions in which the protein assembles only if polymerization inducers are present. Taxol (**1**, Fig. 2, panel A, trace a) and the fluoresceinated taxoid **2** (trace b), in approximately equimolar ratio with tubulin, induced assembly. It was verified by electron microscopy that the generated structures were microtubules (Fig. 2, panel B). Excess of taxoids **1** and **2** does not further increase assembly.[22] In contrast, the acetylated taxoid **3** (trace c) was inactive.

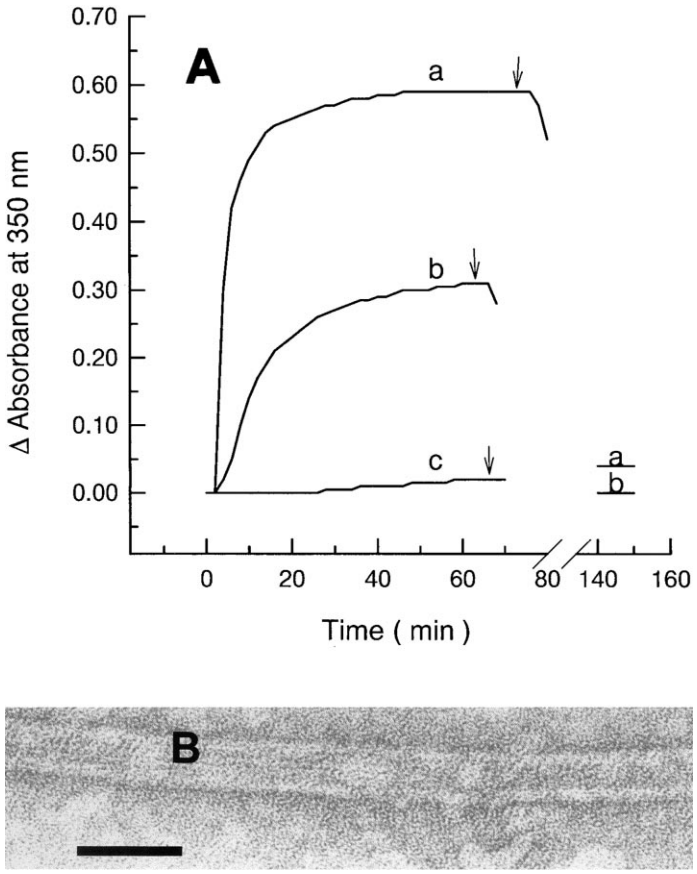

Figure 2. Assembly of purified tubulin 20 μM into microtubules induced by 22 μM taxoids. Taxoids were added at 4 °C and the samples were warmed from 4 to 37 °C at zero time and cooled again as indicated by the arrows (panel A). Trace a, taxol; trace b, taxoid **2**; trace c, taxoid **3**. Panel B shows a representative electron micrograph of one microtubule assembled with **2**. Bar = 50 nm.

The interaction of **2** and **3** with microtubules of the isolated cytoskeletons of PtK2 cells was followed with fluorescence microscopy. Panels A and B of Figure 3 show cytoskeletons prepared by detergent solubilization of the cell plasma membrane. Incubation with **2** (panel A) results in a very neat visualization of the cytoplasmic microtubules, whereas no specific staining occurs with **3** (panel B), but only a weak residual, non-specific labeling of cell nuclei and nucleoli was observed.

Fluorescence microscopy was also used to record the interaction of the taxoids with cells. Incubation of whole cells with **2** (2 h) and glycerol treatment resulted in staining of microtubules and centrosomes (panel C), whereas incubation with **3** gave again non-specific nuclear stain (panel D). The simplest interpretation of the above results is that the acetylation of the 2′-OH group of **2** inactivates the taxoid by suppressing the drug affinity for the microtubule binding site, as noted before for 2′-*O*-acetyltaxol in tubulin solutions.[5,18] Therefore, it can be concluded that the 2′-OH group of the fluorescent taxoid **2** is also essential for the interaction with microtubules at the cell level.

When cells were cultured with **3** for longer periods of time (Fig. 3, panels E and F, 8 h and 24 h, respectively), the fluorescence staining starts to appear, the centrosome being the structure first visualized, followed by the complete microtubule network. This effect was specific of the taxoid binding to the microtubules of the cytoskeleton, as observed with **2** at shorter times (not shown), since the microtubule images can be completely erased by further treatment with an excess of docetaxel, a competing non-fluorescent taxoid (Fig. 3, panel G). The simplest explanation of these results is that **3** is hydrolyzed by the cell culture to taxoid **2**, either by the culture medium or/and by the cells. The first possibility was confirmed by: (i) incubating **3** during 24 h in cell culture medium containing fetal calf serum and treating cytoskeletons with the medium, which gave microtubules images (similarly to panel A of Fig. 3), and (ii) HPLC analysis of the culture medium, which evidenced the

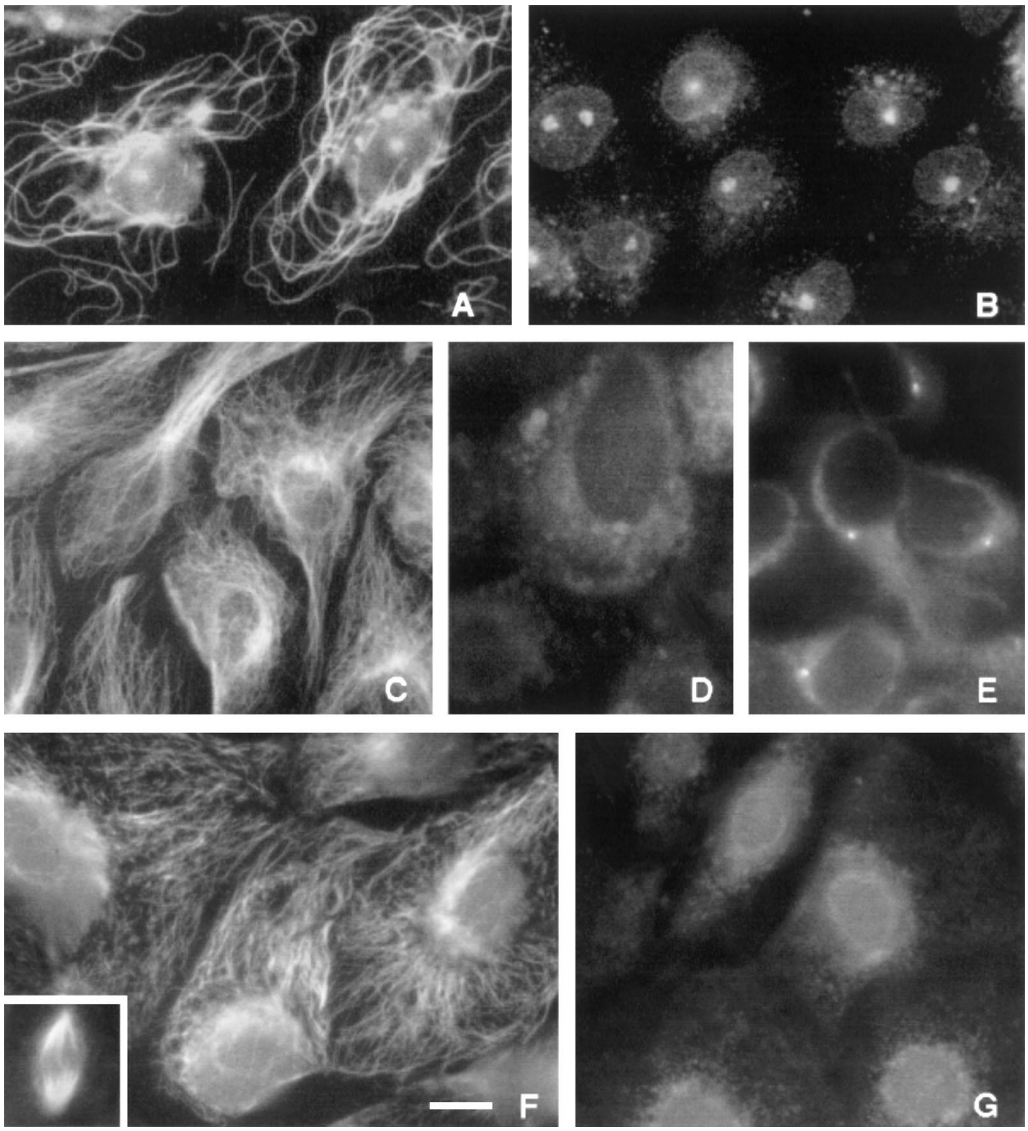

Figure 3. Fluorescence photomicrographs of the comparative binding of taxoids **2** and **3** to microtubules of PtK2 cells. Isolated cytoskeletons: A, B. Whole cells: C–G, observed unfixed (see Experimental). Cytoskeletons were incubated (30 min, room temperature, PEM–PEG buffer) with 1 μM of **2** (panel A) or **3** (panel B). Cells were incubated (37 °C, in reported culture medium) with 1 μM of **2** for 2 h (panel C) or **3** for 2 h (D), 8 h (E), or 24 h (F) (the inset shows the mitotic spindle of a dividing cell). Cells in panel G were treated as in F and further incubated for 5 h after addition of 50 μM docetaxel, that replaced the fluorescent taxoid. Bar = 10 μm.

conversion of **3** to **2** (not shown). These results suggest that **3** could also be hydrolyzed in vivo to **2** in blood plasma, similarly to a prodrug.[7]

Conclusions

The fluorescent taxoids **2** and its 2′-*O*-acetylated derivative **3** present the same collapsed conformation in an aqueous environment, with the groups 2-*O*-benzoyl, 3′-phenyl and 4-*O*-acetyl in close proximity, as deduced from their ^{1}H NMR data. This conformation is also identical to that of the parent drug taxol. Taxoid **2** is fully bioactive, inducing the assembly of tubulin in solution and interacting with individual microtubules and with the cytoskeleton of whole cells, but taxoid **3** is totally inactive, indicating that a free 2′-OH group is essential for cytotoxicity. A slow hydrolysis of the 2′-acetate group of **3** takes place in the cell culture to yield taxoid **2**, the appearance of which, directly observed with fluorescence microscopy for the first time for

an active taxoid, revealed that centrosomes and, later, the microtubules of the cytoskeleton are the structures initially labeled by the bioactive, fluorescent taxoid **2**.

Experimental

7-*O*-[*N*-(4′-Fluoresceincarbonyl)-L-alanyl]taxol (2). It was obtained as described elsewhere.[20] ^{1}H NMR (600 MHz, 3/7 v/v DMSO-d_6/D_2O, 298 K, ref. *H*DO at 4.71 ppm): δ 8.37 (H-3′F), 8.14 (*o*-H of Ph(a)), 8.09 (H-5′F), 7.93 (*o*-H of Ph(c)), 7.88 (*p*-H of Ph(a)), 7.78 (*m*-H of Ph(a)), 7.71 (*p*-H of Ph(c)), 7.62 (*m*-H of Ph(c)), 7.56 (*o*-H of Ph(b), *m*-H of Ph(b)), 7.47 (H-4F, H-5F), 7.36 (*p*-H of Ph(b)), 7.20 (H-1F, H-8F), 6.74 (H-6′F), 6.72 (H-2F, H-7F), 6.40 (H-10), 6.10 (H-13), 5.64 (H-2), 5.60 (H-7), 5.50 (H-3′), 5.20 (H-5), 4.85 (H-2′), 4.64 (C*H* of Ala), 4.35 (H-20a), 4.29 (H-20b), 3.88 (O*H*), 3.68 (H-3), 2.69 (H-6a), 2.41 (4-CH_3CO), 2.30 (10-CH_3CO), 2.01 (H-6b), 1.99 (H-14a), 1.93 (H-18), 1.85 (H-19), 1.76 (H-14b), 1.49 (CH_3 of Ala), 1.20 (H-17), 1.16 (H-16). HPLC analysis as reported.[22]

2′-*O*-Acetyl-7-*O*-[*N*-(4′-fluoresceincarbonyl)-L-alanyl]taxol (3). It was obtained as described for taxoid **2**,[20] but starting from 2′-*O*-acetyltaxol[5] instead of taxol. MS-FAB$^+$ (*m*-nitrobenzyl alcohol), *m*/*z*: 1325.4369 [MH$^+$], (calculated for $C_{73}H_{69}N_2O_{22}$ 1325.4342). ^{1}H NMR (600 MHz, 3/7 v/v DMSO-d_6/D_2O, 298 K, ref. *H*DO at 4.71 ppm): δ 8.31 (H-3′F), 8.12 (*o*-H of Ph(a)), 8.06 (H-5′F), 7.86 (*o*-H of Ph(c)), 7.84 (*p*-H of Ph(a)), 7.76 (*m*-H of Ph(a)), 7.69 (*p*-H of Ph(c)), 7.61 (*m*-H of Ph(c)), 7.57 (*o*-H of Ph(b), *m*-H of Ph(b)), 7.39 (H-4F, H-5F), 7.29 (*p*-H of Ph(b)), 7.15 (H-1F, H-8F), 6.67 (H-6′F), 6.46 (H-2F, H-7F), 6.39 (H-10), 6.00 (H-13), 5.60 (H-2, H-7), 5.49 (H-3′), 5.20 (H-5), 5.59 (H-2′), 4.65 (C*H* of Ala), 4.42 (H-20a), 4.23 (H-20b), 3.80 (H-3), 2.65 (H-6a), 2.42 (4-CH_3CO), 2.25 (10-CH_3CO, 2′-CH_3CO), 1.99 (H-6b), 1.91 (H-14a), 1.90 (H-18), 1.81 (H-19), 1.55 (H-14b), 1.48 (CH_3 of Ala), 1.12 (H-16, H-17). HPLC analysis as reported.[22]

NMR experiments. ^{1}H NMR spectra were obtained at 600 MHz on a Bruker AMX and at 500 MHz on a Varian Unity spectrometer at 298 K in a 3/7 v/v DMSO-d_6/D_2O solution. In this solvent mixture 2–3 mg/mL of fluorescent taxoid could be dissolved. The COSY spectrum was recorded in the absolute mode with a data matrix of 256*1K to digitize a spectral width of 4000 Hz; 16 scans were used with a relaxation delay of 1 s. The 2-D TOCSY experiment was performed using a data matrix of 256*2K to digitize a spectral width of 4000 Hz; 16 scans per increment were used, with a relaxation delay of 2 s. MLEV 17 was used for the 100 ms isotropic mixing time. The 2-D NOESY experiments were performed using a data matrix of 256*2K to digitize a spectral width of 4000 Hz; 16 scans per increment were used with a relaxation delay of 2 s. Mixing times were set at 300, 400, and 500 ms.

Molecular modeling. Initial distance constraints were derived from 100 and 150 ms NOESY spectra. NOEs were translated into distance constraints by visual inspection. Strong, medium and weak cross peaks led to upper bound constraints of 3, 4, and 5 Å, respectively. A pseudoatom correction was also added to the distance limits when a methyl group was involved in the constraint. Lower bounds between non bonded atoms were set to the sum of van der Waals radii. Twenty structures built from the reported coordinates of 7-*O*-[2-(*N*-methyl)pyridinium]taxol acetate[17] were used as input with constraints taken from the NOESY spectra. A simulated annealing was applied to these structures, with the CVFF force field of the INSIGHTII/DISCOVER 95.0 program (Biosym Technologies, USA). After an initial restrained energy minimization (REM) with 5000 conjugate gradient iterations, the structures were heated up to 700 K in 2 ps and, at this temperature, 2 ps of restrained molecular dynamics (RMD) were performed. The structures were then cooled in 100 K steps every 2 ps down to 100 K, where 4 ps of RMD were carried out. The energy of the final structures was minimized (REM) by 10000 conjugate gradient iterations. To test the protocol, the NMR constraints were removed and the structures minimized using up to 5000 conjugate gradient iterations, and no substantial differences were observed. A similar approach, starting from the coordinates reported by Williams et al.,[18] yielded the same results.

Microtubule assembly. Tubulin was purified from calf brain and assembled with taxoids as described elsewhere,[23] with modifications.[24] The protein was equilibrated in 100 mM 2-(*N*-morpholino)ethanesulfonic acid-NaOH buffer, 0.1 mM guanosine triphosphate, pH 6.5, by chromatography in a 0.9×20 cm Sephadex G-25 column at 4 °C. The assembly of microtubules was monitored turbidimetrically at 350 nm in a water-jacketed cell in a Varian 635 spectrophotometer, and by electron microscopy of samples negatively stained with 2% uranyl acetate, in a Phillips EM 400 electron microscope.

Cell experiments. PtK2 mammalian epithelial-like kidney cells were grown and cytoskeletons obtained as described before.[25] Coverslip-attached cells or cytoskeletons were directly mounted without fixation in 0.13 M glycine pH 8.6 buffer containing 0.2 M NaCl and 70% glycerol, and observed through a 63 × Plan-Apochromat objective with a Zeiss Axioplan epifluorescence microscope with fluorescein-specific filters. The images were acquired with a Photometrics 200KAF-1400 cooled

CCD camera and IPLab Spectrum software, and printed with Adobe Photoshop.

Acknowledgements

We thank Dr. L. G. Paloma and Dr. C. S. Swindell for providing access to the coordinates of taxoids, and Dr. M. Bruix for recording the NOESY spectrum of taxoid **2** at 600 MHz. This work was supported by Dirección General de Investigación Científica y Técnica of Spain (Projects PB93-0126, PB95-0116 and PB96-0852, and APC 96-007), by Fundación Científica de la Asociación Española Contra el Cáncer and by Acción Especial C.S.I.C. A.A.S. acknowledges a fellowship from CNPq (Brazil). Taxol® was supplied in part by Bristol-Myers Squibb Inc., the owner of the registered trade name. Docetaxel was provided by Rhone-Poulenc-Rorer.

References and Notes

1. McGuire, W. P.; Hoskins, W. J.; Brady, M. F.; Kucera, P. R.; Partridge, E. E.; Look, K. Y.; Clarke-Pearson, D. L.; Davidson, M. *New Engl. J. Med.* **1996**, *334*, 1.

2. Gelmon, K. *The Lancet* **1994**, *344*, 1267; Rowinsky, E. K.; Donehower, R. C. *New Engl. J. Med.* **1995**, *332*, 1004–1014; Holmes, F. A.; Kudelka, A. P.; Kavanagh, J. J.; Huber, M. H.; Ajani, J. A.; Valero, V. In *Taxane Anticancer Agents. Basic Science and Current Status*; Georg, G. I.; Chen, T. T.; Ojima, I.; Vyas, D. M., Eds.; American Chemical Society: Washington, 1995; pp 31–57; Arbuck, S. G.; Blaylock, B. A. In *Taxol: Science and Applications*; Suffness, M., Ed.; CRC: Boca Raton, 1995; pp 379–415.

3. Schiff, P. B.; Fant, J.; Horwitz, S. B. *Nature (London)* **1979**, *277*, 665; Schiff, P. B.; Horwitz, S. B. *Proc. Natl. Acad. Sci. U.S.A.* **1980**, *77*, 1561; Horwitz, S. B. *Trends Pharm. Sci.* **1992**, *13*, 134; Jordan, M. A.; Wilson, L. In *Taxane Anticancer Agents. Basic Science and Current Status*; Georg, G. I.; Chen, T. T.; Ojima, I.; Vyas, D. M., Eds.; American Chemical Society: Washington, 1995; pp 138–153; Vallee, R. B. In *Taxol: Science and Applications*; Suffness, M., Ed.; CRC: Boca Raton, 1995; pp 259–274.

4. Wani, M. C.; Taylor, H. L.; Wall, M. E.; Coggon, P.; McPhail, A. T. *J. Am. Chem. Soc.* **1971**, *93*, 2325; Guéritte-Voegelein, F.; Guénard, D.; Lavelle, F.; Le Goff, M. T.; Mangatal, L.; Potier, P. *J. Med. Chem.* **1991**, *34*, 992; Swindell, C. S.; Krauss, N.E.; Horwitz, S. B.; Ringel, I. *J. Med. Chem.* **1991**, *34*, 1176; see also the collective volumes *Taxane Anticancer Agents. Basic Science and Current Status*; Georg, G. I.; Chen, T. T.; Ojima, I.; Vyas, D. M., Eds.; American Chemical Society: Washington, 1995; and *Taxol: Science and Applications*; Suffness, M., Ed.; CRC: Boca Raton, 1995.

5. Mellado, W.; Magri, N. F.; Kingston, D. G. I.; Garcia-Arenas, R.; Orr, G. A.; Horwitz, S. B. *Biochem. Biophys. Res. Commun.* **1984**, *124*, 329; Mathew, A. E.; Mejillano, M. R.; Nath, J. P.; Himes, R. H.; Stella, V. J. *J. Med. Chem.* **1992**, *35*, 145.

6. Kant, J.; Huang, S.; Wong, H.; Fairchild, C.; Vyas, D.; Farina, V. *Bioorg. Med. Chem. Lett.* **1993**, *3*, 2471.

7. (a) Nicolaou, K. C.; Riemer, C.; Kerr, M.; Rideout, D.; Wrasidlo, W. *Nature* **1993**, *364*, 464; (b) Georg, G. I.; Boge, T. C.; Cheruvallath, Z. S.; Clowers, J. S.; Harriman, G. C. B.; Hepperle, M.; Park, H. In *Taxol: Science and Applications*; Suffness, M., Ed.; CRC: Boca Raton, 1995; pp 317–375.

8. Hilton, B. D.; Chmurny, G. N.; Muschik, G. M. *J. Nat. Prod.* **1992**, *55*, 1157; Baker, J. K. *Spectrosc. Lett.* **1992**, *25*, 31; Balasubramanian, S. V.; Alderfer, J. L.; Straubinger, R. M. *J. Pharm. Sci.* **1994**, *83*, 1470.

9. Falzone, C. J.; Benesi, A. J.; Lecomte, J. T. J. *Tetrahedron Lett.* **1992**, *33*, 1169.

10. Williams, H. J.; Scott, A. I.; Dieden, R. A.; Swindell, C. S.; Chirlian, L. E.; Francl, M. M.; Heerding, J.; Krauss, N. E. *Can. J. Chem.* **1994**, *72*, 252.

11. Vander Velde, D. G.; Georg, G. I.; Grunewald, G. L.; Gunn, C. W.; Mitscher, L. A. *J. Am. Chem. Soc.* **1993**, *115*, 11650. For a discussion on the conformation analysis of several taxoids see ref 7b.

12. Mastropaolo, D.; Camerman, A.; Luo, Y.; Brayer, G. D.; Camerman, N. *Proc. Natl. Acad. Sci. U.S.A.* **1995**, *92*, 6920.

13. Gao, Q.; Parker, W. L. *Tetrahedron* **1996**, *52*, 2291.

14. Georg, G. I.; Harriman, G. C. B.; Hepperle, M.; Clowers, J. S.; Vander Velde, D. G. *J. Org. Chem.* **1996**, *61*, 2664.

15. Boge, T. C.; Himes, R. H.; Vander Velde, D. G.; Georg, G. I. *J. Med. Chem.* **1994**, *37*, 3337.

16. Ojima, I.; Kuduk, S. D.; Chakravarty, S.; Ourevich, M.; Bégué, J. P. *J. Am. Chem. Soc.* **1997**, *119*, 5519.

17. Paloma, L. G.; Guy, R. K.; Wrasidlo, W.; Nicolaou, K. C. *Chem. Biol.* **1994**, *1*, 107.

18. Williams, H. J.; Moyna, G.; Scott, A. I.; Swindell, C. S.; Chirlian, L. E.; Heerding, J. M.; Williams, D. K. *J. Med. Chem.* **1996**, *39*, 1555.

19. Díaz, J. F.; Menendez, M.; Andreu, J. M. *Biochemistry* **1993**, *32*, 10067; Andreu, J. M.; Díaz, J. F.; Gil, R.; de Pereda, J. M.; García de Lacoba, M.; Peyrot, V.; Briand, C.; Towns-Andrews, E.; Bordas, J. *J. Biol. Chem.* **1994**, *269*, 31785.

20. Souto, A. A.; Acuña, A. U.; Andreu, J. M.; Barasoain, I.; Abal, M.; Amat-Guerri, F. *Angew. Chem. Int. Ed. Engl.* **1995**, *34*, 2710.

21. Guy, R. K.; Scott, Z. A.; Sloboda, R. D.; Nicolaou, K. C. *Chem. Biol.* **1996**, *3*, 1021.

22. Evangelio, J. A.; Abal, M.; Barasoain, I.; Souto, A. A.; Lillo, M. P.; Acuña, A. U.; Amat-Guerri, F.; Andreu, J. M. *Cell Motil. Cytoskel.* **1998**, *39*, 73.

23. Andreu, J. M.; Gorbunoff, M. J.; Lee, J. C.; Timasheff, S. N. *Biochemistry* **1984**, *23*, 1742.

24. Díaz, J. F.; Andreu, J. M. *Biochemistry* **1993**, *32*, 2747.

25. De Inés, C.; Leynadier, D.; Barasoain, I.; Peyrot, V.; García, P.; Briand, C.; Rener, G. A.; Temple, C. *Cancer Res.* **1994**, *54*, 75.